rameters, it is X that seems to provide the most objective information on polymer local structure in the studied system, since this parameter is least correlated to the other parameters of the model. In our opinion, Moynihan's approach is a valuable tool in the analysis of the effect of delicate differences in molecular or supermolecular structure on relaxation properties of heterogeneous polymeric materials.

Registry No. polystyrene (homopolymer), 9003-53-6.

References and Notes

(1) Kobeko, P. P. "Amorphous Substances"; Moscow, Leningrad, 1952 (in Russian).
(2) Kovacs, A. J. *Fortschr. Hochpolym.-Forsch.* **1963**, *3*, 394.
(3) Shen, M. C.; Eisenberg, A. *Prog. Solid State Chem.* **1966**, *3*, 407.
(4) Gibbs, J. H. In "Modern Aspects of the Vitreous State"; Mackenzie, J. D., Ed.; Butterworths: London, 1960; vol. 1, p 152.
(5) Hirai, N.; Eyring, H. *J. Polym. Sci.* **1959**, *37*, 51.
(6) Kanig, G. *Kolloid Z. Z. Polym.* **1969**, *233*, 54.
(7) Volkenstein, M. V.; Ptitsyn, O. B. *Zh. Tekh. Fiz.* **1956**, *26*, 2204.
(8) Wolpert, S. M.; Weitz, A.; Wunderlich, B. *J. Polym. Sci., Polym. Phys. Ed.* **1971**, *9*, 1887.
(9) Chen, F. C.; Choy, C. L.; Wong, S. P.; Young, K. *Polymer* **1980**, *21*, 1139.
(10) Chow, T. S.; Prest, W. M., Jr. *J. Appl. Phys.* **1982**, *53*, 6568.
(11) Kovacs, A. J.; Aklonis, J. J.; Hutchinson, J. M.; Ramos, A. R. *J. Polym. Sci., Polym. Phys. Ed.* **1979**, *17*, 1097.
(12) Davies, R. O.; Jones, G. O. *Adv. Phys.* **1953**, *2*, 370.
(13) Moynihan, C. T.; Easteal, A. J.; DeBolt, M. A.; Tucker, J. *J. Am. ceram. Soc.*, **1976**, *59*, 12.
(14) DeBolt, M. A.; Easteal, A. J.; Macedo, P. B.; Moynihan, C. T. *J. Am. ceram. Soc.* **1976**, *59*, 16.
(15) Hodge, I. M.; Huvard, G. S. *Macromolecules* **1983**, *16*, 371.
(16) Hodge, I. M. *Macromolecules* **1983**, *16*, 898.
(17) Demchenko, S. S.; Privalko, V. P.; Lipatov, Yu. S. *Vysokomol. Soedin.*, in press.
(18) Boyer, R. *Rubber Chem. Technol.* **1963**, *36*, 1303.
(19) Marshall, A. S.; Petrie, S. E. B. *J. Appl. Phys.* **1975**, *46*, 4223.
(20) O'Reilly, J. M. *J. Appl. Phys.* **1979**, *50*, 6083.
(21) O'Reilly, J. M. In "Studies in Physical and Theoretical Chemistry", Walton, A. G.; Ed.; Elsevier: Amsterdam, 1980; vol. 10, 165.
(22) Berry, G. C.; Fox, T. G. *Adv. Polym. Sci.* **1968**, *5*, 261.
(23) Privalko, V. P.; Besklubenko, Yu. D.; Lipatov, Yu. S.; Demchenko, S. S.; Khmelenko, G. I. *Vysokomol. Soedin., Ser. A.* **1977**, *19*, 1744.
(24) Privalko, V. P.; Titov, G. V. *Vysokomol. Soedin., Ser. A.*, **1979**, *21*, 348.
(25) Lipatov, Yu. S. "Physical Chemistry of Filled Polymers"; Khimia: Moscow 1977 (in Russian).

Polymer-Supported Catalysis: Stereoselective Oxidation of L-Dopa by Iron(III) Complex Ions Anchored to Asymmetric Polymers

B. Pispisa* and A. Palleschi

Dipartimento di Chimica, Università di Napoli, 80134 Naples, Italy, and Dipartimento di Chimica, Università di Roma, 00185 Rome, Italy. *Received May 17, 1985*

ABSTRACT: $[Fe(tetpy)(OH)_2]^+$ ions anchored to sodium poly(L-glutamate) or sodium poly(D-glutamate) were used as catalysts for the H_2O_2 oxidation of L-dopa at pH 7 (tetpy = 2,2′:6′,2″:6″,2‴-tetrapyridyl). The catalytic sequence involves (a) formation of a substrate–catalyst precursor complex, (b) intramolecular electron transfer within this intermediate, and (c) oxidation of both the lower valence metal chelate and dopa radical by H_2O_2 in subsequent fast steps. Stereoselective phenomena are observed only when the formation of the diastereomeric precursor complexes is assisted by the ordered polypeptide matrices. The conformational asymmetry of the polymers ensures different steric constraints for LL and DL adducts, which are thought to affect differently the mutual orientation and separation distance of the redox centers, in agreement with the finding that chiral discrimination is chiefly observed in step b. A hypothetical model of the diastereomeric noncovalent electron-transfer complexes was constructed by conformational energy calculations. The models are consistent with a number of experimental findings and support the hypothesis that stereoselectivity is coupled with a remote attack mechanism on the central metal ion. Implications of the stereochemical features of the catalytic systems on the efficiency of reaction are also discussed.

Introduction

Second-order rate constants of outer-sphere redox processes are expressible as products of the equilibrium quotient for the formation of a precursor complex (K_0, M^{-1}) and the unimolecular specific rate for the electron-transfer step (k_{et}, s^{-1}), when this latter is rate-determining.[1] In a very few cases, however, it has been proved possible to resolve the observed rate constants into their elementary components,[2,3] because no saturation kinetics are often observable.[1b] Furthermore, in all but few instances[4,5] redox reactions between pairs of achiral species have been studied, despite the fact that the use of optically active compounds could have some relevance for biological processes as well as for practical purposes.

We have recently shown that the H_2O_2 oxidation of L(+)-ascorbic acid (I) and L-adrenaline (II) catalyzed by hemin-like $[Fe(tetpy)(OH)_2]^+$ ions (tetpy = 2,2′:6′,2″:6″,2‴-tetrapyridyl) anchored[6] to sodium poly(L-glutamate) (FeTL) or sodium poly(D-glutamate) (FeTD) proceeds stereoselectively only when the formation of the diastereomeric precursor complexes is assisted by the ordered polymeric matrices.[7] Stereoselectivity ratios (k_{DL}/k_{LL}) around 4 were then obtained, corresponding to an enantiomeric excess of about 65%. Moreover, kinetic data in the steady-state conditions allowed us to evaluate k_{et} and K_0,[7b,c] and the product $k_{et}K_0$ was found to be in

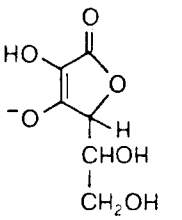

(I)

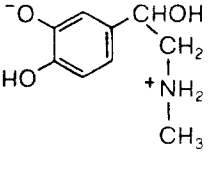

(II)

0024-9297/86/2219-0904$01.50/0

satisfactory agreement with the observed specific rates (k_{DL} and k_{LL}, $M^{-1}\cdot s^{-1}$). It was then possible to prove that stereoselectivity is almost entirely kinetically controlled, the ratio $k_{et,DL}/k_{et,LL}$ being definitely higher than K_{0DL}/K_{0LL}.

We now present the results of the oxidation of L-dopa (3,4-dihydroxyphenylalanine) by the FeTL or FeTD system, under the same experimental conditions, according to the reaction[8]

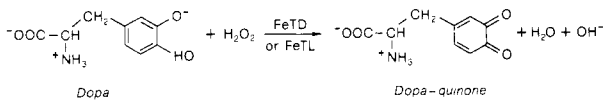

Evidence is produced that stereoselectivity is quite comparable to that obtained with the other substrates, despite the fact that the chiral center is differently removed from the reacting OH groups. Furthermore, kinetic effects were still found to be largely responsible for the observed phenomena. A hypothetical model of the diastereomeric noncovalent electron-transfer complexes shall be also presented. The models are based on conformational energy calculations and supported by experimental results, as far as the limited data allow. They show that the redox centers in the diastereomeric adducts experience a different mutual orientation and separation distance.

Experimental Section

Materials. *trans*-$[Fe(tetpy)(OH)_2]^+$ complex ions, sodium poly(L-glutamate), and sodium poly(D-glutamate) were obtained as already described.[7,9] Concentrations of the complex, polymers, and L-dopa were determined by UV absorption at 300 (ϵ = 13 430), 200 (ϵ = 5500), and 280 nm (ϵ_{max} = 2720 $M^{-1}\cdot cm^{-1}$) (pH 7). Polymer concentration [P] is referred to the monomeric unit (monomol/L). Tris buffer (Sigma) was employed in the chloride form and in the concentration of 0.05 M (pH 7.01 ± 0.03). Under the experimental conditions used, the degree of association of FeT ions by polyelectrolytes is higher than 93% according to equilibrium dialysis experiments.[6b] L-Dopa (Merck) and stabilizer-free H_2O_2 (Erba) were analytical-grade reagents and used without further purification. All measurements were carried out on freshly prepared solutions, using doubly distilled water.

Methods. The stoichiometry of the overall reaction (see Introduction) was checked by titration of 5×10^{-4} M dopa with H_2O_2, monitoring the absorbance at 475 nm due to dopaquinone[8a] (λ_{max} = 304 and 475 nm, ϵ_{475} = 4500 $M^{-1}\cdot cm^{-1}$), at this wavelength the absorbance of 2×10^{-5} M catalyst (referred to FeT) being negligible (ϵ = 580 $M^{-1}\cdot cm^{-1}$, pH 7). As a result, the mean of $[dopa]_{reacted}/[H_2O_2]_{consumed}$ was 0.9 ± 0.1, suggesting a 1:1 stoichiometry for the reaction.

Kinetic experiments measuring the formation of dopaquinone at 320 or 475 nm were ordinarily carried out under pseudo-first-order conditions with respect to H_2O_2 and at fixed pH (7; 0.05 M Tris buffer). A typical run consisted of adding hydrogen peroxide by a microsyringe into the 1-cm optical cell containing 2 mL of catalyst and substrate, both systems being thermostated at 26.0 ± 0.1 °C. The experimental conditions were as follows: $[H_2O_2] = 1 \times 10^{-2}$ M, $[AH^-] = 2 \times 10^{-4}$ M, $[C] = 0.5 \times 10^{-5}$–5×10^{-5} M and [C]/[P] = 0.01–0.20, AH^-, C, and P denoting substrate, complex ions, and polypeptides, respectively. Measurements were also carried out at 16 and 13 °C without practically affecting the α-helical content in the polypeptide matrices.[7a] Plots of log ($A_t - A_\infty$) vs. t were normally linear over more than 80% of the reaction progress, and the observed rate constants were obtained from the slopes.

Under the experimental conditions used, dopaquinone undergoes a rearrangement reaction[8a] with initial rates about 40–80 times slower than those of its formation, i.e., $\sim 5 \times 10^{-9}$ as compared to (2–5) $\times 10^{-7}$ $M\cdot s^{-1}$. For instance, when $[AH^-] = 2 \times 10^{-4}$, $[C] = 5 \times 10^{-5}$ M, and [C]/[P] = 0.04 (FeTD), the initial rates were 4.7×10^{-9} and 4.3×10^{-7} $M\cdot s^{-1}$, respectively, a factor of 90 difference in the rates being thus observed. In the few cases when deviation from linearity in log (absorbance) vs. t plots occurred at around, or below 2 half-lives, nonlinear least-squares calculations for consecutive first-order reactions[10] were carried out to obtain k_{obsd} (s^{-1}). (The mean value of the rate constant of dopaquinone transformation, calculated by this method for a number of runs under different conditions, is (1.45 ± 0.12) $\times 10^{-4}$ s^{-1}, while ϵ = 4500 ± 200 $M^{-1}\cdot cm^{-1}$, to be compared with (1.5 ± 0.2) $\times 10^{-4}$ and 4100 ± 300, as experimentally determined at 475 nm.)

Four kinetic measurements were performed for each run to obtain consistency in the results. At each [C]/[P] ratio investigated, plots of k_{obsd} against complex concentration always gave straight lines and the second-order rate constants of the catalysis k_{DL} and k_{LL} ($M^{-1}\cdot s^{-1}$) were obtained from the slopes. The rate constants of the complex-ion-uncatalyzed oxidation of L-dopa ($k_{0,app}$, $M^{-1}\cdot s^{-1}$) were obtained from plots of k_0 (s^{-1}) as a function of $[H_2O_2]_0$ under second-order conditions ($[H_2O_2]_0/[AH^-]_0 \sim 1$).

Initial reaction velocities, $V_0 = -d[AH^-]/dt$ ($M\cdot s^{-1}$), at different [C]/[P] ratios and fixed $[C]_0$ were evaluated from the slope of the dopaquinone concentration against time curves at $t \to 0$, the extent of dopa oxidation being generally limited to about 20% of the original concentration. In agreement with the literature,[8] dopa in aqueous buffered or complex-free poly(glutamate) solutions does not practically undergo oxidation, even in the presence of hydrogen peroxide.

Absorption measurements were carried out on a Beckman DBGT or a Cary 219 spectrophotometer. Circular dichroism spectra were recorded on a Cary 61 instrument with appropriate quartz cells. Calorimetric data were obtained by a LKB 10700-2 batch microcalorimeter at 25 °C. Other apparatuses were already described.[7]

Results and Discussion

Kinetics and Reaction Mechanism. Typical kinetic data of the oxidation of L-dopa (AH^-) at pH 7 (0.05 M Tris buffer) and $[H_2O_2]_0/[AH^-]_0$ = 50 are shown in Figure 1, where the observed pseudo-first-order specific rates k_{obsd} (s^{-1}) are plotted as a function of complex concentration [C] at fixed [C]/[P] = 0.01 and 0.20 (26 °C). The linear variation of rate with the concentration of polymer-supported FeT ions indicates true catalytic behavior for the iron(III) compound. Furthermore, at all [C]/[P] ratios investigated the straight lines have intercepts that differ from 0; i.e., $k_{obsd} = k_0 + k_{cat}[C]$, where $k_{cat} = k_{DL}$ or k_{LL} depending upon the chirality of the catalytic system.

When second-order conditions with respect to H_2O_2 were adopted ($[H_2O_2]_0/[AH^-]_0 \approx 1$), the slopes of the straight lines were found to remain practically constant, within experimental errors, whereas the intercepts increase with increasing $[H_2O_2]_0$, as shown in Figure 2 for [C]/[P] = 0.10.

From the results, the following empirical rate expression may be formulated:

$$-\frac{d[AH^-]}{dt} = k_{0,app}[H_2O_2][AH^-] + k_{cat}[C][AH^-] \quad (1)$$

The dependence of $k_{0,app}$ and k_{cat} on [C]/[P] is illustrated in Figure 3.[11]

These findings are reminiscent of those obtained with both L-ascorbic acid and L-adrenaline (Table I) and indicate the occurrence of parallel pathways.[7] One of these ($k_{0,app}$) refers to an "uncatalyzed" electron-transfer process from dopa to hydrogen peroxide and the other (k_{cat}) to a catalytic $[H_2O_2]$-independent route to products, whose rate-determining step involves one molecule of substrate per molecule of complex ion.

Inspection of Figure 3 shows that (1) stereoselectivity of both catalytic and complex-ion-uncatalyzed reactions increases with increasing [C]/[P] ratio, that of the former being definitely higher than that of the latter, however (for instance, at [C]/[P] = 0.20, k_{DL}/k_{LL} = 4.0 ± 0.3 while $k_{0,D,app}/k_{0,L,app}$ = 1.5 ± 0.2), and (2) stereoselectivity occurs at the expense of the catalytic efficiency because the rate constants markedly decrease as the [C]/[P] ratio increases.

If the ellipticity at 220 nm of sodium poly(L-glutamate) in the presence of complex ions is plotted against [C]/[P]

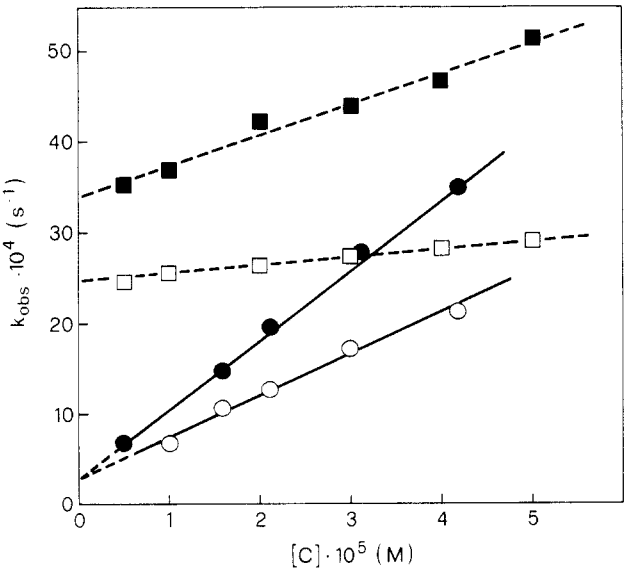

Figure 1. Catalytic effect for the oxidation of L-dopa in the presence of FeTL (open symbols) or FeTD (solid symbols) enantiomeric system at [C]/[P] = 0.01 (solid lines) or 0.20 (broken lines) and 26.0 °C; pH 7 (0.05 M Tris buffer); $[AH^-]_0 = 2 \times 10^{-4}$ M; $[H_2O_2]_0 = 1 \times 10^{-2}$ M.

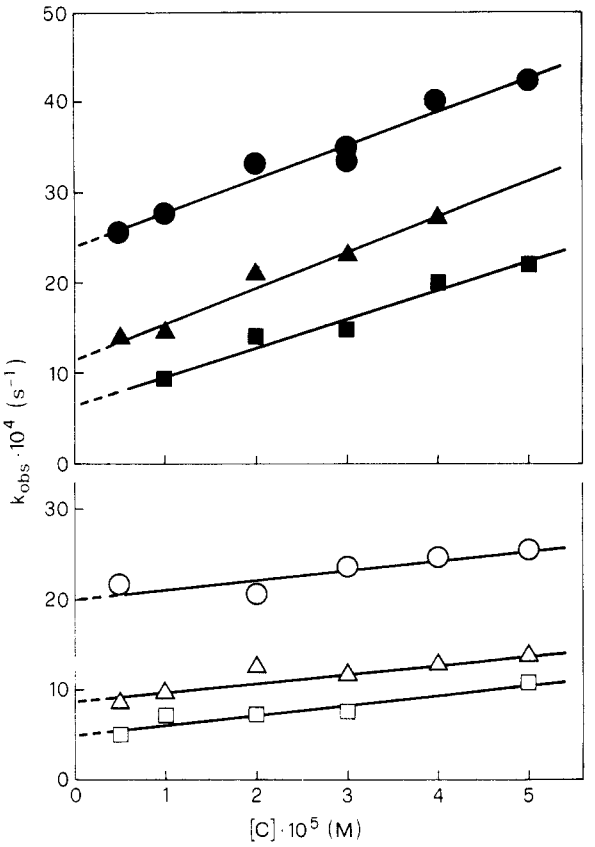

Figure 2. Catalytic effect for the oxidation of L-dopa in the presence of FeTL (open symbols) or FeTD (solid symbols) enantiomeric system at [C]/[P] = 0.10 and varying initial concentrations of hydrogen peroxide. $[H_2O_2]_0 = 1 \times 10^{-2}$ M (circles), 2×10^{-4} M (triangles) and 1×10^{-4} M (squares). Other experimental conditions are as in Figure 1.

together with both the stereoselectivity ratio (k_{DL}/k_{LL}) and activation energy (E_a) of the catalysis, an S-shaped curve is obtained (Figure 4). This trend clearly indicates the very existence of a relationship between binding-induced conformational phenomena in the polypeptide matrices by FeT ions[6] and chiral discrimination in the oxidation

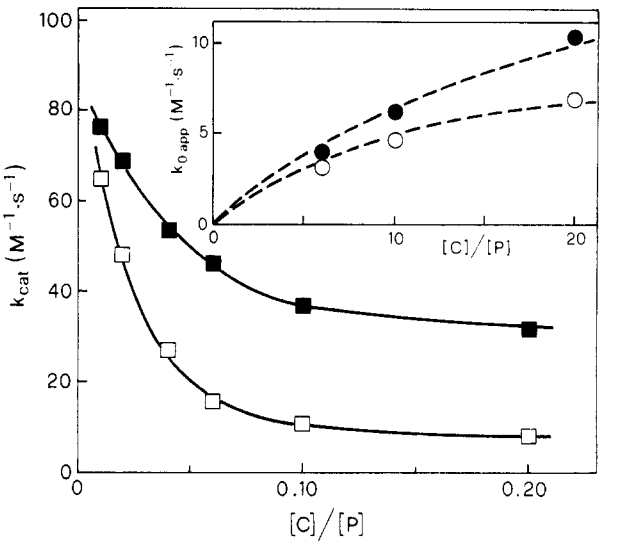

Figure 3. Dependence of second-order rate constants for the oxidation of L-dopa catalyzed by FeTL (open symbols) or FeTD (solid symbols) system on complex to polymer residue ratio. T = 26.0 °C; pH 7 (0.05 M Tris buffer). The solid lines are calculated according to eq 3 (see text). Insert: variation of second-order rate constant for the complex-ion-uncatalyzed oxidation of L-dopa in FeTL or FeTD solutions (open and solid symbols, respectively) as a function of [C]/[P] ratio, under the same experimental conditions.

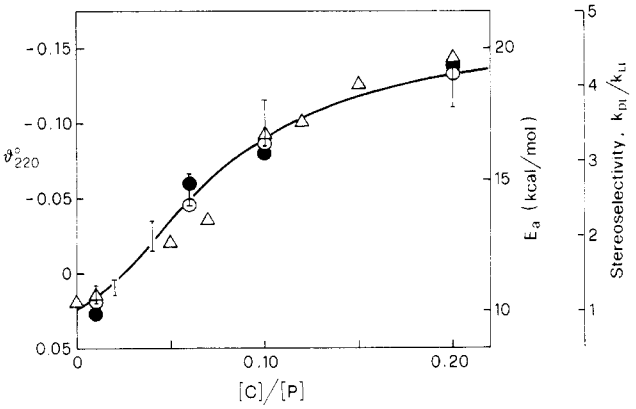

Figure 4. Variation of ellipticity at 220 nm (△) of sodium poly(L-glutamate) 7.5×10^{-4} M in the presence of FeT ions and of stereoselectivity (vertical bars) and activation energy (circles) of the catalytic oxidation of L-dopa by the FeTL (open symbols) or FeTD (solid symbols) system as a function of complex to polymer residue ratio. T = 26 °C; pH 7. Measurements of ellipicity were normalized for an optical path length of 1 cm.

process of L-dopa. The extrinsic ellipticity at 287 nm of bound achiral FeT ions exhibits the same trend.

We next investigated the dependence of the initial rate of the reaction on the initial concentration of dopa, at fixed complex concentration and varying [C]/[P] ratio. Under pseudo-first-order conditions with respect to hydrogen peroxide, saturation kinetics were observed. Since, under these conditions, the initial rate of reaction can be written as $V_0 = k_0[AH^-] + V_{cat}$, V_{cat} may be evaluated by knowing k_0 from independent measurements (see above). A typical double-log plot of V_{cat} as a function of $[AH^-]_0$, at $[C]_0 = 2 \times 10^{-5}$ M, is shown in Figure 5. As expected from the foregoing kinetic results, the rate of catalysis strictly follows a first-order saturation curve at low substrate concentration, i.e., the slope is unitary, while at high dopa concentration all curves show the tendency toward saturation. This suggests that the catalytic oxidation of dopa occurs via the formation of a precursor complex in a preequilibrium step and that electron transfer from the substrate to

Table I
Second-Order Rate Constants for the Oxidation of L-Ascorbic Acid and L-Adrenaline at Different [C]/[P] Ratios[a]

substrate	[C]/[P]	k_{DL}, $M^{-1}\cdot s^{-1}$	k_{LL}, $M^{-1}\cdot s^{-1}$	k_{DL}/k_{LL}[b]	$k_{0,D,app}$, $M^{-1}\cdot s^{-1}$	$k_{0,L,app}$, $M^{-1}\cdot s^{-1}$	$k_{0,D,app}/k_{0,L,app}$[c]
L-(+)-ascorbic acid	0.01	3705 ± 116	3608 ± 119	1.0			
	0.10	442.3 ± 42.9	153.6 ± 12.6	2.9 ± 0.4	230.6 ± 24.0	157.0 ± 14.7	1.5 ± 0.2
	0.20	414.0 ± 33.4	106.4 ± 9.2	3.9 ± 0.5	287.8 ± 26.2	156.0 ± 14.8	1.8 ± 0.2
L-adrenaline	0.01	158.0 ± 7.6	159.9 ± 8.8	1.0			
	0.10	29.7 ± 1.8	9.4 ± 0.8	3.1 ± 0.3	3.4 ± 0.3	2.5 ± 0.2	1.4 ± 0.2
	0.20	31.2 ± 2.1	7.5 ± 0.5	4.2 ± 0.4	4.9 ± 0.5	3.2 ± 0.3	1.5 ± 0.2

[a] At 25.9 °C, pH 7, 0.05 M Tris buffer, $[AH^-]_0 = 1 \times 10^{-4}$ M. [b] Stereoselectivity ratio of the catalysis. [c] Stereoselectivity ratio of the complex-ion-uncatalyzed oxidation of substrates.

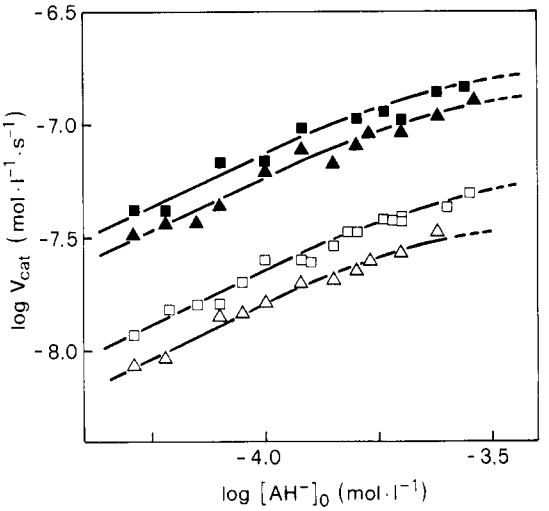

Figure 5. Reaction velocity of the catalytic oxidation of L-dopa as a function of the initial concentration of substrate, at a fixed complex ion concentration of 2×10^{-5} M. Catalytic system: FeTL (open symbols) or FeTD (solid symbols) at [C]/[P] = 0.10 (squares) or 0.20 (triangles). T = 25.9 °C, pH 7 (0.05 M Tris buffer), and $[H_2O_2]_0 = 1 \times 10^{-2}$ M.

iron(III) takes place intramolecularly within the intermediate, i.e.

$$Fe^{III}TL^+ \text{ (or } FeTD^+) + AH^- \underset{k_{-1}}{\overset{k_1}{\rightleftharpoons}} Fe^{III}TLAH$$

$$Fe^{III}TLAH \xrightarrow[\text{(slow)}]{k_{et}} Fe^{II}TL + AH\cdot$$

$$Fe^{II}TL + {}^1/_2H_2O_2 \xrightarrow[\text{(fast)}]{} Fe^{III}TL^+ + OH^-$$

$$AH\cdot \text{ (or } A^-\cdot + H^+) + {}^1/_2H_2O_2 \xrightarrow[\text{(fast)}]{} A + H_2O$$

$$AH\cdot + A^- \xrightarrow[\text{(fast)}]{} AH^- + A$$

where $Fe^{III}TL^+$ denotes FeT ions bound to poly(L-glutamate). The scheme predicts that a fast oxidation of the reduced iron ion and dopa radical by H_2O_2 follows the electron-transfer step, which is rate-determining. AH· (or $A^-\cdot$) may also disproportionate, as does ascorbate radical.[7a]

According to the data of Figure 5, V_{cat} (i.e., the electron-transfer rate between dopa and the central metal ion) may be expressed as

$$V_{cat} = \frac{k_{et}K_0[C]_0[AH^-]}{1 + K_0[AH^-]} \qquad (2)$$

where $K_0 = k_1/k_{-1}$. Straight lines are, therefore, obtained by plotting V_{cat}^{-1} against $[AH^-]^{-1}$, having intercept $I = (k_{et}[C]_0)^{-1}$ s·M^{-1} and tangent $T = (k_{et}K_0[C]_0)^{-1}$ s^{-1}. From the results, one obtains (by least-squares using V^2 weight factors) the values of k_{et} and K_0 shown in Figure 6. They are of the same order of magnitude of those reported for the oxidation of dopa by copper–poly(lysine)[5] and of *p*-

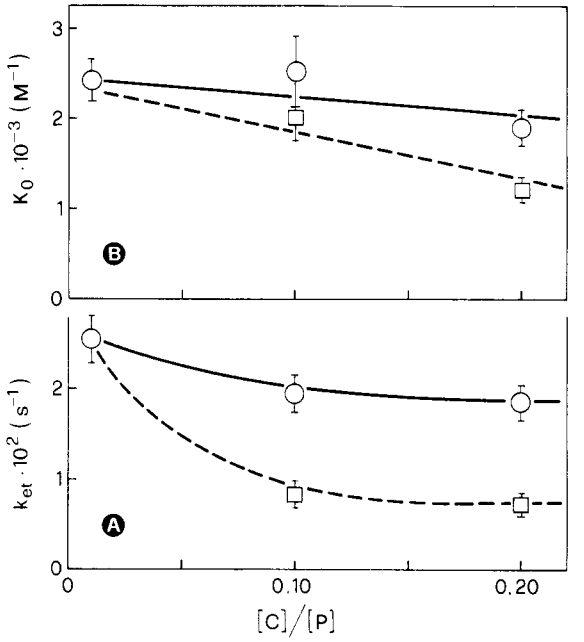

Figure 6. Variation of the unimolecular rate constant for electron transfer from L-dopa to the central metal ion (A) and of the equilibrium constant for the formation of precursor complex (B) as a function of complex to polymer ratio of FeTL (squares) or FeTD (circles) catalytic system (see text). The experimental conditions are as in Figure 5.

Table II
Kinetic and Thermodynamic Stereoselectivity in the Electron Transfer from L-Dopa to Iron(III) in the FeTL or FeTD system[a]

[C]/[P]	$k_{et,DL}/k_{et,LL}$	$K_{0,DL}/K_{0,LL}$	$(k_{et,DL}/k_{et,LL})$ $(K_{0,DL}/K_{0,LL})^b$	k_{DL}/k_{LL}[b]
0.01	~1	~1	~1	1.2 ± 0.2
0.10	2.3 ± 0.4	1.2 ± 0.3	2.8 ± 0.8	3.5 ± 0.3
0.20	2.6 ± 0.4	1.5 ± 0.2	3.9 ± 0.8	4.0 ± 0.3

[a] At 25.9 °C, pH 7, 0.05 M Tris buffer. [b] Overall stereoselectivity.

hydroquinone and homogentisic acid by copper–poly(histidine).[12] When $K_0[AH^-] \ll 1$, eq 2 reduces to $V_{cat} = k_{et}K_0[C]_0[AH^-] = k_{cat}[C][AH^-]$ (see eq 1). Comparison of $k_{et}K_0$ with k_{cat} is rather satisfactory, a finding that substantiates the foregoing mechanism. For instance, $(k_{et}K_0)_{DL} = 61.2 \pm 7.7$ as compared to $k_{DL} = 76.3 \pm 4.4$ $M^{-1}\cdot s^{-1}$ at [C]/[P] = 0.01, and $(k_{et}K_0)_{DL} = 33.7 \pm 5.3$ and $(k_{et}K_0)_{LL} = 8.7 \pm 1.3$ $M^{-1}\cdot s^{-1}$ as compared to $k_{DL} = 31.4 \pm 2.1$ and $k_{LL} = 7.9 \pm 0.4$ $M^{-1}\cdot s^{-1}$ at [C]/[P] = 0.20. Furthermore, stereoselectivity appears to be largely controlled by kinetic effects, i.e., $k_{et,DL}/k_{et,LL} > K_{0,DL}/K_{0,LL}$ (Table II).

Differential calorimetric measurements[13] on FeTL–L-dopa against FeTD–L-dopa ([C]/[P] = 0.20, 25 °C) deaerated mixtures substantiate the foregoing results. The energetics of chiral discrimination was found to be around 150 cal/mol, under conditions where the association of

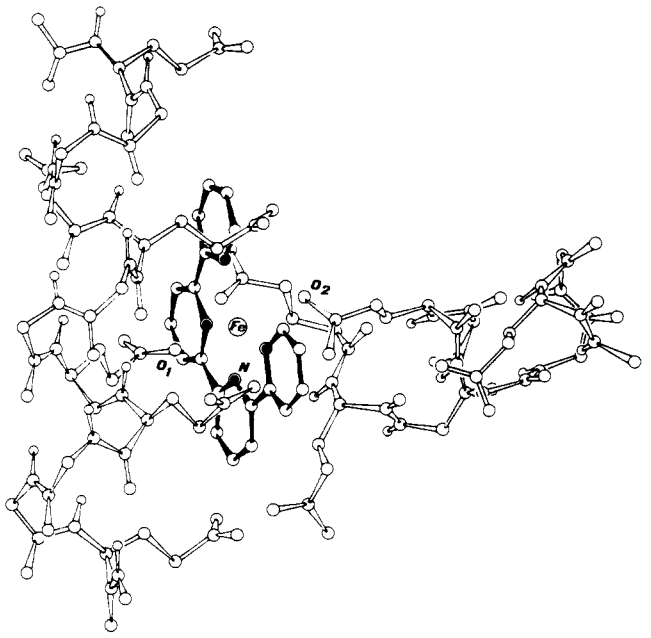

Figure 7. Molecular model of the FeTL catalyst, under conditions where it exhibits stereoselective activity (see text). The oxygen atoms of the side chains of poly(L-glutamate) closest to Fe(III) are indicated as O_1 and O_2. They lie on the axis normal to the equatorial plane of the complex, at a separation distance of 2.35 and 2.50 Å from the central metal ion, respectively.

substrate is virtually complete. This figure is of the order of magnitude that one would have expected on the basis of $K_{0,DL}/K_{0,LL}$ value (Table II), on the reasonable assumption that the entropies of association of the diastereomeric pairs are nearly identical.

Structural Features of Catalysts and Chiral Discrimination. The overall results may be rationalized by taking into account the structural features of the catalytic systems. (Quaterpyridine)iron(III) ions form an inner-sphere complex with the polyelectrolyte, whose γ-carboxylate groups act as unidentate ligands.[6] Furthermore, with increasing [C]/[P] ratio both a coil-to-α-helix transition in the polypeptide matrices (Figure 4) and aggregation phenomena, where FeT ions very likely act as bridging groups between helical segments of different chains or of the same chain after partial folding, occur.[7b,14] Therefore, if specific steric requirements have to be met in order to observe stereoselective effects in the catalysis, they are matched only by increasing the [C]/[P] ratio because the low accessibility of the active centers makes the chiral residues of the ordered polymer behave as primary sites of binding for substrate molecules. The ultimate result should be the rise of a chiral discrimination in the electron-transfer step since the conformational asymmetry of polypeptides ensures different steric constraints for the diastereomeric adducts, affecting differently the orientation and separation distance of the redox centers.[15,17] This is indeed the case, as shown in Figure 6 and Table II.

The most relevant structural features of the FeTL catalyst at high [C]/[P] ratio, i.e., under conditions where it exhibits stereoselective activity, are illustrated in Figure 7. The molecular model was obtained by conformational energy calculations, partially based on available X-ray data, in the deepest minimum of the total interaction energy given as a sum of electrostatic and nonbonded energy terms.[18]

Competitive Catalytic Pathways. The observation that stereoselectivity occurs at the expense of the efficiency of catalysis may be explained in terms of competitive routes to products, depending on the structural characteristics of FeTL and FeTD systems. This hypothesis agrees with the foregoing considerations and is supported by the results shown in Figure 4 and the finding that the dependence of k_{cat} on X = [C]/[P] ratio is satisfactorily describable by the empirical expression

$$k_{cat} = k' \frac{1}{1 + aX^2} + k'' \frac{aX^2}{1 + aX^2} \qquad (3)$$

where k' is the specific rate at $X \rightarrow 0$, k'' is the (limiting) rate constant at high values of X (where k_{cat} exhibits an almost asymptotic value and stereoselectivity approaches the maximum value), and a is an adjustable constant. The data of Figure 3 were, in fact, fitted with an average deviation of 5% (solid lines in the figure), which is of the same order of magnitude of the standard deviations of k_{cat}, using $k' = 80\ M^{-1}\cdot s^{-1}$ with both enantiomeric systems and $k''_D = 31.1$ and $k''_L = 7.3\ M^{-1}\cdot s^{-1}$. (Constant a was 7.83×10^2 and 2.00×10^3, respectively.)

According to eq 3, we may consider the reactant molecules to be divided into two groups that follow parallel pathways. In one group would be those molecules that are oxidized with specific rate k', irrespective of the chirality of the catalytic systems. This fraction, designated $(1 + aX^2)^{-1}$, is obviously the larger the lower X is. Under these conditions, FeT ions are bound to the random coil polypeptides and exhibit an "open" (axial) position that very likely represents the site of interaction for the catecholic oxygen ion of the substrate,[10,19] in agreement with spectroscopic data.[14] Electron transfer from dopa to the central metal ion can thus take place directly, but a small stereoselectivity is expected because of the high conformational mobility of this type of adduct.[20] This is indeed the case, as shown in Figures 1 and 3 and in Table II. In the other group would be those substrate molecules that are oxidized with rate constants k''_D and k''_L, depending on the enantiomeric system employed. This fraction, designated $[(aX^2)(1 + aX^2)^{-1}]$, predominates at high values of X, i.e., when the substrate–catalyst adduct involves primarily the ordered polymer because aggregation of helical chains hinders the accessibility of the catalytic centers (see above). In such a case, only a remote attack mechanism on the iron(III) can occur, probably making use of the π system of the peripheral tetrapyridyl ligand of the active sites.[21] The tendency by which L-dopa is converted to dopaquinone depends, therefore, on competition between nonstereospecific and stereospecific pathways in the overall catalytic cycle. Consequently, it is not surprising that the rate of catalysis decreases as stereoselectivity rises (Figure 3).

Conformational Analysis. The conformational order and rigidity of polypeptide chains in solution provide a good opportunity for investigating the foregoing topochemical effects by conformational energy calculations. The main purpose of these calculations was to know the geometrical and steric constraints that control the formation of the diastereomeric adducts undergoing stereoselective electron transfer.

In past years, conformational energy calculations[22,23] or computational studies[24,25] on reaction complexes of biologically significant species have been carried out by giving a good insight into the stereochemistry of such complexes and the reaction pathway.

The formation of the diastereomeric adducts undergoing stereoselective reaction was examined by conformational energy calculations based on two types of van der Waals potential functions, together with electrostatic and hydrogen bonding energy terms. The total conformational

Table III
Molecular Parameters of the Diastereomeric Noncovalent Electron-Transfer Models and Calculated Stereoselectivity

reductant	diaster	NB[a]	$\bar{R}$[b]	R_0[c]	R'[d]	$\Delta U_{tot}(R)$[e]	stereoselectivity calcd[f,g]	stereoselectivity calcd[f,h]	stereoselectivity exptl[i]	ref[j]
	DL	B	7.1	2.9	7.2	60 ± 80	4.3 ± 0.8	2.6 ± 0.5		27
	LL	B	5.8	3.2	7.5					
	DL	B′	6.9	2.9	7.1	40 ± 70	4.1 ± 0.8	2.5 ± 0.4		28
L-dopa	LL	B′	5.7	3.0	7.5					
	DL	LJ	7.0	2.9	7.1	70 ± 85	4.3 ± 0.8	2.7 ± 0.5		29
	LL	LJ	5.8	3.1	7.5					
	DL	LJ′	7.0	2.9	7.1	70 ± 90	4.1 ± 0.8	2.6 ± 0.4		30
	LL	LJ′	5.9	3.1	7.5					
ave	DL		7.0 ± 0.1		7.1 ± 0.1	60 ± 90	4.2 ± 0.8	2.6 ± 0.5	3.9 ± 08	
	LL		5.8 ± 0.1		7.5 ± 0.1					
	DL	B	7.1	2.8	7.5	250 ± 160	4.4 ± 0.7	4.7 ± 0.7		27
	LL	B	7.6	3.1	7.8					
	DL	B′	7.0	2.8	7.5	330 ± 180	5.1 ± 1.0	5.3 ± 0.8		28
L-adrenaline	LL	B′	7.4	3.1	7.8					
	DL	LJ	7.0	2.7	7.5	280 ± 160	4.6 ± 0.9	4.8 ± 0.7		29
	LL	LJ	7.5	3.1	7.8					
	DL	LJ′	7.0	2.7	7.5	120 ± 110	3.4 ± 0.7	3.7 ± 0.5		30
	LL	LJ′	7.6	3.1	7.8					
ave	DL		7.0 ± 0.1		7.5 ± 0.1	245 ± 185	4.3 ± 0.8	4.6 ± 0.7	4.5 ± 1.1	
	LL		7.5 ± 0.1		7.8 ± 0.1					

[a] Nonbonding potentials used in eq 5 (see text). [b] Closest catecholic O⁻···Fe separation distance (Å) in the deepest minimum of total energy. [c] (Closest) catecholic O⁻···C-tetrapyridyl separation distance (Å). [d] Catecholic O⁻···Fe separation distance (Å) via tetrapyridyl ring, based on the molecular geometry of the models. [e] $U_{LL} - U_{DL}$ in cal/mol. [f] Overall stereoselectivity calculated according to eq 5. [g] Using $\bar{R}$ values. [h] Using R' values. [i] 25.9 °C, pH 7, 0.05 M Tris buffer, [C]/[P] = 0.20. [j] For NB potentials.

energy of the substrate–catalyst (red–ox) complex was calculated as the sum of all pairwise nonbonded, electrostatic, and hydrogen bonding interactions, the internal coordinates of both partners being those obtained by minimizing the internal conformational energy given as a sum of nonbonded and electrostatic energy terms.[22] For the purpose, the following general equation was used:

$$U_{tot}(R_{ij}) = \sum_{i \neq j} \left[\frac{A_{ij} \exp(-B_{ij}R_{ij})}{R_{ij}^{\,d}} - \frac{C_{ij}}{R_{ij}^{\,6}} \right] + \sum_{i \neq j} \frac{z_i z_j e^2}{D_s R_{ij}(1 + kR_{ij})} + \sum_{i \neq j} \frac{D'}{R_{ij}^{\,3}} \quad (4)$$

where the first term refers to nonbonding interactions, the second term refers to electrostatic interactions, and the third one is a dipole–dipole function that takes into account hydrogen-bonding interactions between NH_2^+ or NH_3^+ or hydroxyl groups of the substrate and carboxylic groups of the catalytic system ($D' = -55$ kcal·Å^3·mol^{-1}).[26] When $d = 0$ in the first term of eq 4, we denote the nonbonding potential as B, and when $B_{ij} = 0$ and $d = 12$ we denote it as LJ (see Table III). Furthermore, ze in the Coulombic expression is the monopole charge, D_s the static dielectric constant of the solvent (set equal to 78.5), and k the inverse of the Debye–Hückel screening length (0.07 at 25 °C and $\mu = 0.04$ M). In all cases, R_{ij} is the separation distance of the pertinent atoms i and j.

A preliminary account of these calculations was already reported,[18] but we now have completed a thorough study on conformational analysis of the diastereomeric adducts, using four different sets of values for the interatomic interaction parameters A_{ij}, B_{ij}, and C_{ij} in the nonbonding potentials of eq 4.[27-30]

Structural Features of Catalyst–Substrate Adducts. Calculations were performed by keeping the catalytic system rigidly fixed and allowing the substrate to undergo only rigid-body (translational and rotational) motion. We searched for the deepest minimum in the total energy in terms of both the six degrees of freedom of the approaching molecule and the closest separation distance between catecholic O⁻ and iron(III). Several minimizations were carried out by starting from different mutual orientations of the reactants as well as different directions of approach of L-dopa or L-adrenaline.

As a general observation, it appears that the most sterically favorable direction for the entering substrate molecules is always the same, irrespective of the chirality of the catalyst. The formation of precursor complexes in the systems investigated is, therefore, characterized by a specific pathway, reminiscent of that observed when substrate molecules approach the prosthetic group of metalloenzymes. In addition, it appears that both L-dopa and L-adrenaline and the enantiomeric catalytic systems fit together in the close environment of the active sites with remarkable precision, leaving no gaps at the intermolecular interface. The reduction of the local dielectric constant that results from solvent exclusion as the molecules associate should enhance the electrostatic free energy of binding, giving rise to a further stabilization of the adducts.[31] This effect has been recently shown to increase dramatically the binding free energy of reaction complexes[25] and may explain the relatively high values of K_0 illustrated in Figure 6.

The geometrical features of FeTL–L-dopa and FeTD–L-dopa interaction complexes, as obtained by conformational energy calculations in the deepest minimum of total energy (see above), are shown in Figure 8, and those of the same complexes with L-adrenaline are illustrated in Figure 9. The most relevant molecular parameters of these hypothetical electron-transfer adducts are summarized in Table III together with the overall calculated stereoselectivity of the reaction.

Correlation of Stereoselectivity with the Molecular Parameters of Models. Stereoselectivity was evaluated by the equation

$$(k_{DL}/k_{LL}) = (R_{DL}/R_{LL})^2 \exp[(U_{LL} - U_{DL})/RT](k_{et,DL}/k_{et,LL}) \quad (5)$$

where R is the closest catecholic O⁻ ··· Fe separation distance (denoted as $\bar{R}$) in the deepest minimum of total interaction energy or is the same separation distance calculated via tetrapyridyl ring on the basis of the molecular geometry of the models (and it is denoted as R'),

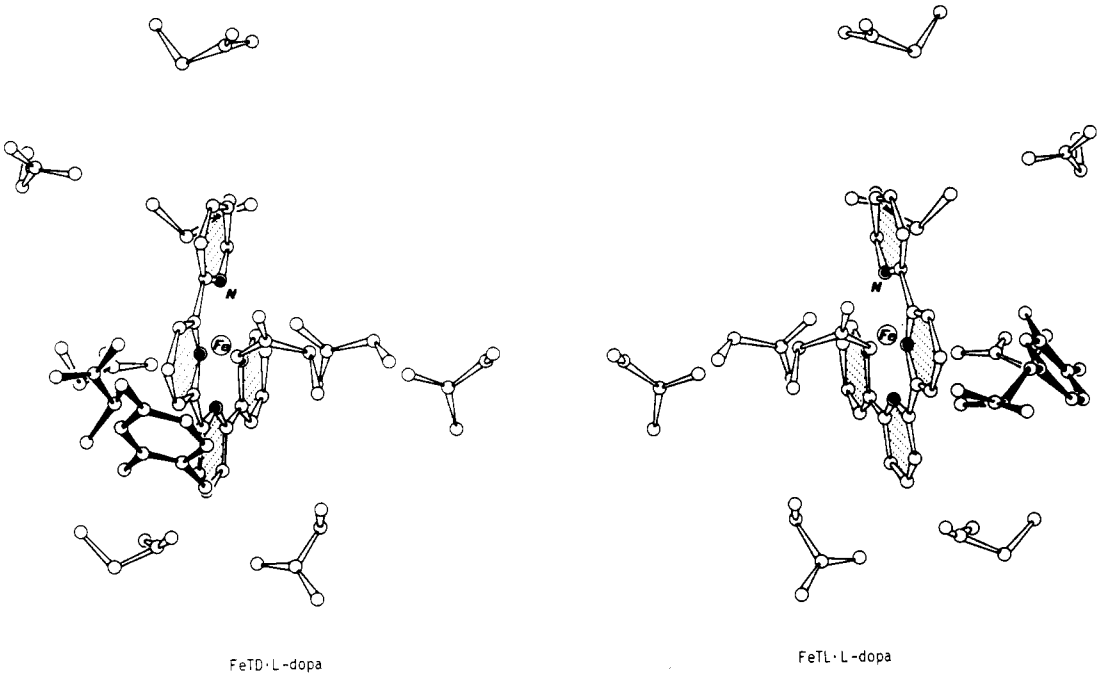

Figure 8. Hypothetical FeTD·L-dopa (left) and FeTL·L-dopa (right) electron-transfer complexes, undergoing stereoselective reaction. For clarity, only the side chains of the polypeptide nearest to the active site are shown.

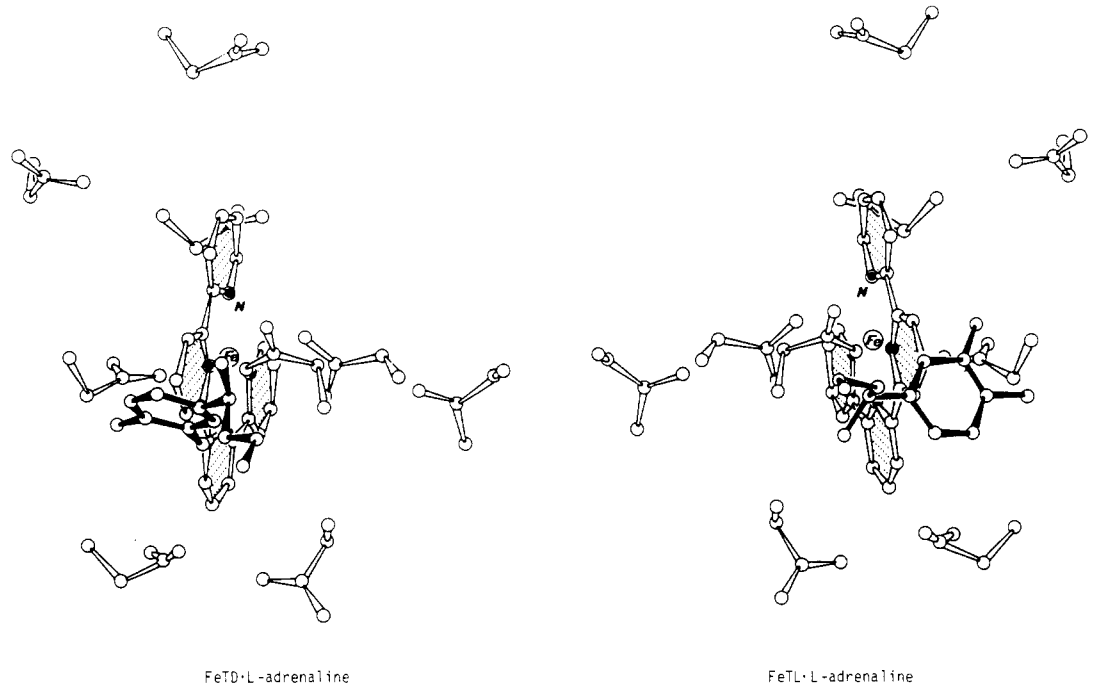

Figure 9. Hypothetical FeTD·L-adrenaline (left) and FeTL·L-adrenaline (right) electron-transfer complexes, undergoing stereoselective reaction. For clarity, only the side chains of the polypeptide nearest to the active site are shown.

($U_{LL} - U_{DL}$) is the difference in the total intermolecular energy at $\bar{R}$ (or R') for the diastereomeric pairs, as obtained by the foregoing calculations, and k_{et} is the specific rate of the intramolecular electron-transfer step. Equation 5 may be justified as follows. The equilibrium constant for the formation of precursor complex in outer-sphere electron-transfer processes between spherically symmetric reactants in dilute solution is approximately expressible as[15,17,32,33]

$$K_0 = A \exp(-W/RT) \tag{6}$$

where $W = W(\bar{R}_{kl}) - RT \ln F(R_{kl},\theta)$, $W(\bar{R}_{kl})$ being the work (not only or necessarily Coulombic[16b]) required to bring the reactants together at the "effective" encounter distance $\bar{R}_{kl}$ (often considered to be the contact distance of the reacting species[15,17]), $F(R_{kl},\theta)$ being a switching function to be discussed below, and A being the statistical part of the stability constant. A is given by $4\pi C\bar{R}_{kl}^2\,\delta R$ and corresponds to the probability of finding the reactant pairs separated by a distance between $\bar{R}_{kl}$ and $\bar{R}_{kl} + \delta$R, on the assumption that δR is small enough so that $\exp[-W(\bar{R}_{kl})/RT] \approx \exp[-W(\bar{R}_{kl} + \delta R)/RT]$, and C is a conversion factor (6.023×10^{-4}) to express K_0 in the usual way (M^{-1}) when R_{kl} is in Å. The function F may vary from 1 for a strictly spherically symmetric system (hard spheres) to a value much less than 1 when, say, interpenetration of reactants occurs through a preferential direction (for steric reasons) or the accessibility of reactant molecules is partially hindered so that a reduced surface is available for the process.[34]

According to the foregoing kinetic results (i.e., $k_{cat} = K_0 k_{et}$) and the above considerations, eq 5 was straightforwardly obtained on the assumption that δR and F are practically the same for the diastereomeric adducts. This assumption is nearly valid in that the fraction F of the orientational phase space of FeT ions that is sterically accessible at the reactants separation R', estimated from the molecular geometry of the models, varies of no more than 15% in going from one diastereoisomer to the other.[36] It must be also noted that eq 5 relies on the energy difference of the diastereomeric pairs so as to overcome the uncertainty in the absolute value of the total interaction energy that arises from the empirical terms of eq 4.

When stereoselectivity calculated with $\bar{R}$ or R' values is compared with that experimentally determined, a rather satisfactory agreement is observed for both substrates with all nonbonding potential functions employed (Table III). In contrast, when the molecular parameters of diastereomeric pairs corresponding to other relative minima of the total interaction energy were taken into account, a very poor agreement between calculated and experimental stereoselectivity is obtained.[37] Moreover, if one compares the values of $(U_{LL} - U_{DL})$ reported in Table III with those of $(\Delta H_{LL} - \Delta H_{DL})$, as determined under conditions where the association of substrates by the catalytic systems at [C]/[P] = 0.20 is virtually complete, a surprisingly good agreement is observed both in magnitude and sign. The energetics of chiral discrimination in the reactions investigated were, in fact, found to be 150 ± 40 for L-dopa and 250 ± 60 cal/mol for L-adrenaline.[13] It also appears from the preexponential factor of eq 5 that the difference in the entropies of association of the diastereomeric pairs is negligibly small, as one would predict if the modes of binding are similar.[38]

All these findings make it reasonable to consider the present hypothetical models as a good representation of the actual diastereomeric electron-transfer complexes.

Correlation of Stereoselectivity with Activation Process. When the free energy change required to reach the activated complex from the precursor complex $[\Delta G_{et}^{\ddagger} = RT \ln (k_B T/hk_{et})]$ of the diastereomeric reactions with L-dopa and L-adrenaline[7b] is plotted against $1/R'$, a straight line is roughly obtained with slope 40 ± 12 kcal·Å·mol^{-1}, which is rather close to the theoretical value (see below). This implies that a major determinant of chiral discrimination in the kinetic process is the outer-sphere (solvent) reorganization energy because it is related to the encounter distance of the redox species.[15,16] In fact, according to Marcus theory, the inner-sphere reorganization energy is likely to be constant for the diastereomeric precursor complexes while the standard free energy changes $[\Delta(\Delta G^{\circ\prime}) = \Delta(\Delta G^{\circ}) + \Delta(W^{p}) - \Delta(W^{r})$, where ΔG° is the standard free energy of the elementary electron-transfer step and W^{r} and W^{p} are work terms for bringing the reactants together and for separating the products, respectively[16]] are expected to be small (see above). Since the radii of reactants are also constant for the series considered here,[36] the Marcus free energy barrier for the intramolecular electron transfer reduces, as a first approximation, to (25 °C)[1,15,16]

$$\Delta G^{*} = \text{const} - [(e^2/4R')(D_{op}^{-1} - D_s^{-1})] = \text{const} - 45/R' \quad (7)$$

where D_{op} and D_s are the optical and static dielectric constants of the medium. Then $\Delta G^{\ddagger} = I - T/R'$, with T = 45 kcal·Å·mol^{-1}, because $\Delta G^{\ddagger} = \Delta G^{*} - RT \ln (hZ/k_B T)$,[13,16] Z being the collision frequency (usually taken to be 10^{13} s^{-1} [40]). Considering the assumptions and approximations, the agreement between experimental and theoretical slopes appears acceptable.[41] Whether orbital overlap considerations are also important for the chiral discrimination, especially in view of the significant differences in the mutual orientation of the reactants in the diastereomeric pairs (Figures 8 and 9), remains to be seen.[1,15a,17,40]

Concluding Remarks

To summarize, depending upon the structural features of the enantiomeric catalytic systems, the oxidation of L-dopa and similar substrates[7] can proceed by direct or remote attack on the central metal ion, each pathway leading to quite different stereoselective effects because of the different stereochemical characteristics of the precursor complexes.

The models of the diastereomeric noncovalent electron-transfer adducts, as obtained by conformational energy calculations, are fully consistent with experimental data showing that chiral discrimination is coupled with a remote attack mechanism. They also emphasize the role played by the ordered polypeptide matrices in controlling kinetic stereoselectivity that predominates in the reactions investigated.

Acknowledgment. We thank Professors P. De Santis and G. Nemethy for helpful discussions. Financial support by MPI (Rome) is gratefully acknowledged.

Registry No. L-Dopa, 59-92-7; L-(+)-ascorbic acid, 50-81-7; L-adrenaline, 51-43-4.

References and Notes

(1) Sutin, N. In "Tunneling in Biological Systems"; Chance, B., De Vault, D. C., Frauenfelder, H., Marcus, R. A., Schrieffer, J. R., Sutin, N., Eds.; Academic Press: New York, 1979; p 201.; *Acc. Chem. Res.* **1982**, *15*, 275.
(2) Gaswick, D. G.; Haim, A. *J. Am. Chem. Soc.* **1971**, *93*, 7347. Haim, A.; Sutin, N. *Inorg. Chem.* **1976**, *15*, 476.
(3) Eley, C. G. S.; Ragg, E.; Moore, G. R. *J. Inorg. Biochem.* **19844**, *21*, 295.
(4) Grossman, B.; Wilkins, R. G. *J. Am. Chem. Soc.* **1967**, *89*, 4230. Sutter, J. H.; Hunt, J. B. *Ibid.* **1969**, *91*, 3107. Kane-Maguire, N. A. P.; Tollison, R. M.; Richardson, D. E. *Inorg. Chem.* **1976**, *15*, 499. Geselowitz, D. A.; Taube, H. *J. Am. Chem. Soc.* **1980**, *102*, 4525.
(5) Hatano, M.; Nozawa, T.; Ikeda, S.; Yamamoto, T. *Makromol. Chem.* **1971**, *141*, 11. Nozawa, T.; Hatano, M. *Ibid.* **1971**, *141*, 31.
(6) (a) Branca, M.; Marini, M. E.; Pispisa, B. *Biopolymers* **1976**, *15*, 2219. (b) Branca, M.; Pispisa, B. *J. Chem. Soc., Faraday Trans. 1* **1977**, *73*, 213.
(7) (a) Barteri, M.; Pispisa, B. *J. Chem. Soc., Faraday Trans. 1* **1982**, *78*, 2073, 2085. (b) Pispisa, B.; Barteri, M.; Farinella, M. *Inorg. Chem.* **1983**, *22*, 3166. (c) Pispisa, B.; Farinella, M. *Biopolymers* **1984**, *23*, 1465.
(8) (a) Heacock, R. A. *Chem. Rev.* **1959**, *59*, 181. (b) Martin, R. B. *J. Phys. Chem.* **1971**, *75*, 2657.
(9) Branca, M.; Pispisa, B.; Aurisicchio, C. *J. Chem. Soc., Dalton Trans.* **1976**, 1543. Cerdonio, M.; Mogno, F.; Pispisa, B.; Romani, G. L.; Vitale, S. *Inorg. Chem.* **1977**, *16*, 400.
(10) Alcock, N. W.; Benton, D. J.; Moore, P. *Trans. Faraday Soc.* **1970**, *66*, 2210.
(11) Comparison between observed and calculated overall reaction velocity is rather satisfactory. For example, at [C]/[P] = 0.10, $k_{0,D,app}$ = 6.1 ± 0.6, and $k_{0,L,app}$ = 4.8 ± 0.4 M^{-1}·s^{-1}, whereas k_{DL} = 36.1 ± 4.4 and k_{LL} = 10.3 ± 0.9 M^{-1}·s^{-1}. When $[H_2O_2]_0 = 1 \times 10^{-4}$, $[AH^-]_0 = 2 \times 10^{-4}$, and [C] = 2×10^{-5} M, the calculated initial rates are $V_{DL} = 2.66 \times 10^{-7}$ and $V_{LL} = 1.37 \times 10^{-7}$ M·s^{-1} as compared to 2.29×10^{-7} and 1.14×10^{-7} M·s^{-1}, respectively.
(12) Pecht, I.; Levitzki, A.; Anbar, M. *J. Am. Chem. Soc.* **1967**, *89*, 1587.
(13) Paradossi, G.; Pispisa, B.; Rizzo, R.; Barteri, M. *Biopolymers*, in press.
(14) Pispisa, B. In "The Coordination Chemistry of Metalloenzymes"; Bertini, I., Drago, R. S., Luchinat, C., Eds.; Reidel: Dordrecht, 1983; NATO Advanced Institute Series, p 279.
(15) (a) Sutin, N. *Prog. Inorg. Chem.* **1983**, *39*, 441. (b) Brown, G. M.; Sutin, N. *J. Am. Chem. Soc.* **1979**, *101*, 883.

(16) (a) Marcus, R. A. *Discuss. Faraday Soc.* **1960**, *29*, 21; *Annu. Rev. Phys. Chem.* **1964**, *15*, 155. (b) *J. Chem. Soc., Faraday Discuss.* **1982**, *74*, 7.
(17) Newton, M. D. *Int. J. Quantum Chem., Quantum Chem. Symp.* **1980**, *14*, 363; *ACS Symp Ser.* **1982**, *198*, 255.
(18) Pispisa, B.; Palleschi, A.; Barteri, M.; Nardini, S. *J. Phys. Chem.* **1985**, *89*, 1767.
(19) Gergely, A.; Kiss, T. In "Metal Ions in Biological Systems"; Sigel, H., Ed.; Dekker: New York, 1979; Vol. 9, p 143.
(20) Hwang, F.-J.; De Bolt, L. C.; Morawetz, H. *J. Am. Chem. Soc.* **1976**, *98*, 5890.
(21) Castro, C. E.; Davis, N. F. *J. Am. Chem. Soc.* **1969**, *91*, 5405. Sutin, N.; Forman, A. *Ibid.* **1971**, *93*, 5274. Toppen, D. L. *Ibid.* **1976**, *98*, 4023. Hanson, L. K.; Chang, C. K.; Davis, M. S.; Fajer, J. *Ibid.* **1981**, *103*, 663.
(22) Pincus, M. R.; Scheraga, H. A. *Acc. Chem. Res.* **1981**, *14*, 299.
(23) De Tar, D. F. *J. Am. Chem. Soc.* **1981**, *103*, 107.
(24) Poulos, T. L.; Kraut, J. *J. Biol. Chem.* **1980**, *255*, 10322.
(25) Matthew, J. B.; Weber, P. C.; Salemme, F. R.; Richards, F. M. *Nature (London)* **1983**, *301*, 169.
(26) Whittington, S. G. *Biopolymers* **1971**, *10*, 1481.
(27) Calascibetta, F. G.; Dentini, M.; De Santis, P.; Morosetti, S. *Biopolymers* **1975**, *14*, 1667.
(28) Abe, A.; Mark, J. E. *J. Am. Chem. Soc.* **1976**, *98*, 6468.
(29) Brant, D. A.; Flory, P. J. *J. Am. Chem. Soc.* **1965**, *87*, 2791. Brant, D. A. *Macromolecules* **1968**, *1*, 291.
(30) Momany, F. A.; Carruthers, L. M.; McGuire, R. F.; Scheraga, H. A. *J. Phys. Chem.* **1974**, *78*, 1595.
(31) Friedman, H. L. *Pure Appl. Chem.* **1981**, *53*, 1277.
(32) Hupp, J. T.; Weaver, M. J. *J. Phys. Chem.* **1984**, *88*, 1463.
(33) Tembe, B. L.; Friedman, H. L.; Newton, M. D. *J. Chem. Phys.* **1982**, *76*, 1490. Logan, J.; Newton, M. D. *Ibid.* **1983**, *78*, 4086.
(34) Examples of $F \ll 1$ are reported for redox reactions either when small molecules interact with metalloenzymes, where the active site is normally "buried" in the protein,[35] or even when simple complex ions interpenetrate each other to make shorter the center-to-center distance.[17,33]
(35) Sutin, N. In "Inorganic Biochemistry"; Eichhorn, G. L., Ed.; Elsevier: Amsterdam, 1973; Vol. 2, p 611. Mauk, A. G.; Scott, R. A.; Gray, H. B. *J. Am. Chem. Soc.* **1980**, *102*, 4360.
(36) Calculations were carried out by approximating the reactants to spheres, as usually done,[15b] of radius 3.7 (dopa), 3.8 (adrenaline), and 5.7 Å (FeT). In the latter case, we used the relation $\bar{r} = {}^1/_2(d_1d_2d_3)^{1/3}$, where the d_i are the "diameters" along the three L–Fe–L axes.[15b] Values of d_i were estimated from molecular models and known crystallographic data. For py–Fe–Py and (C)O–Fe–O(C) diameters, the values used were 14.1 and 7.4 Å, respectively, having also taken into account the van der Waals radius of the "external" hydrogen atom in pyridine and of carbon atoms in –O(C). The choice of a more realistic (oblate spheroid) model for the bound FeT ions ($l_a = l_b = 7.1$ and $l_c = 3.7$ Å) makes the average F value for the four diastereomeric pairs at the reactants separation R', estimated from the molecular geometry of the models, somewhat larger, being approximately 0.10 ± 0.01 as compared to 0.06 ± 0.01.[18] The F_{DL}/F_{LL} ratio does not change appreciably, however (about 1.14 for L-dopa and 1.12 for L-adrenaline).
(37) For instance, other relative minima were found at a catecholic $O^-\cdots$Fe separation distance of 7.6 and 7.4 Å for DL and LL complex with dopa and 8.3 and 8.0 Å for the same complexes with adrenaline, $(U_{LL} - U_{DL})$ being –280 and –410 cal/mol, respectively. With these values in eq 5, it comes out a calculated stereoselectivity of 1.7 for both substrates.
(38) Since $k_{cat} = K_0k_{et} = A \exp(-W/RT)(k_BT/h) \exp(-\Delta G_{et}^{\ddagger}/RT)$,[15b] the overall free energy of activation is expressible as $\Delta G^{\ddagger} = \Delta G_{et}^{\ddagger} + \bar{W} - RT \ln F - RT \ln A$ (see eq 6). When $\delta F/\delta T = 0$ is assumed, the overall activation entropy is given by $\Delta S^{\ddagger} = -\delta(\Delta G^{\ddagger})/\delta T = \Delta S_{et}^{\ddagger} - \delta\bar{W}/\delta T + R \ln F + R \ln A + RT(\delta \ln A/\delta T)$, and then $(\Delta S_{LL}^{\ddagger} - \Delta S_{DL}^{\ddagger}) = (\Delta S_{etLL}^{\ddagger} - \Delta S_{etDL}^{\ddagger}) - [(\delta\bar{W}_{LL}/\delta T) - (\delta\bar{W}_{DL}/\delta T)] - R \ln (F_{DL}/F_{LL}) - R \ln (A_{DL}/A_{LL}) + RT(\delta \ln A_{LL}/\delta T) - (\delta \ln A_{DL}/\delta T)]$. The second and last term of this equation should be very close to 0 so that the difference in the entropies of association of the diastereomeric pairs is essentially given by $[-R \ln (F_{DL}/F_{LL}) - 2R \ln (R'_{DL}/R'_{LL})] = 0 \pm 1$ cal/(mol·deg).[36] For each pair, the entropy effects due to reduction of molecular degrees of freedom is probably overbalanced by those arising from solvent release, however.[25,39]
(39) Pispisa, B.; Paoletti, S. *J. Phys. Chem.* **1980**, *84*, 24.
(40) Marcus, R. A. In "Tunneling in Biological Systems" (see ref 1); p 109.
(41) That the outer-sphere reorganization energy plays an important role in the observed phenomena may also be inferred from the following considerations. Since $R' < (\bar{r} + a)$, $\bar{r}$ and a being the radii of the reactants,[36] a more realistic model for electron transfer over medium distance is that in which the two interacting species fill an ellipsoidal cavity in the solvent.[33,42] Then the solvent reorganization energy has the form:[15a,43] $\Delta G^*_{out} = [45R'^2/2l_a'l_b'^2]S$ kcal/mol), where S is a "shape" function that takes into account the eccentricity of the ellipsoid[42,43] and l_a' and l_b' are the semimajor and semiminor axes. These axes are fixed by the following constraints: (i) V(ellipsoid) = V(FeT) + V(substr), where V denotes volume, and (ii) $l_a' = {}^1/_2(R' + \bar{r} + a)$, on the assumption of an average symmetrical configuration about the foci. Then we obtain $(\Delta G_{LL}^* - \Delta G_{DL}^*)_{out} = 0.4$ and 0.3 kcal/mol for L-dopa and L-adrenaline, respectively, as compared to $(\Delta G_{LL}^{\ddagger} - \Delta G_{DL}^{\ddagger})_{et} = 0.6$ and 0.7 kcal/mol. Similar $\Delta(\Delta G_{out}^*)$ values were estimated with the oblate spheroid model for the oxidant rather than the spherical one,[36] but the interfocal distances were about 2 Å larger.
(42) Ehrenson, S. *J. Am. Chem. Soc.* **1976**, *98*, 7510.
(43) Cannon, R. D. *Chem. Phys. Lett.* **1977**, *49*, 299; "Electron Transfer Reactions"; Butterworth: London, 1980; Chapter 6.